



HAL
open science

Global 4DVAR Assimilation and Forecast Experiments Using AMSU Observations over Land. Part II: Impacts of Assimilating Surface-Sensitive Channels on the African Monsoon during AMMA

Fatima Karbou, Florence Rabier, Jean-Philippe Lafore, Jean-Luc Redelsperger, Olivier Bock

► **To cite this version:**

Fatima Karbou, Florence Rabier, Jean-Philippe Lafore, Jean-Luc Redelsperger, Olivier Bock. Global 4DVAR Assimilation and Forecast Experiments Using AMSU Observations over Land. Part II: Impacts of Assimilating Surface-Sensitive Channels on the African Monsoon during AMMA. *Weather and Forecasting*, 2010, 25, pp.PP.20-36. 10.1175/2009WAF2222244.1 . meteo-00463557

HAL Id: meteo-00463557

<https://meteoFrance.hal.science/meteo-00463557v1>

Submitted on 2 Nov 2021

HAL is a multi-disciplinary open access archive for the deposit and dissemination of scientific research documents, whether they are published or not. The documents may come from teaching and research institutions in France or abroad, or from public or private research centers.

L'archive ouverte pluridisciplinaire **HAL**, est destinée au dépôt et à la diffusion de documents scientifiques de niveau recherche, publiés ou non, émanant des établissements d'enseignement et de recherche français ou étrangers, des laboratoires publics ou privés.



Distributed under a Creative Commons Attribution 4.0 International License



Global 4DVAR Assimilation and Forecast Experiments Using AMSU Observations over Land. Part II: Impacts of Assimilating Surface-Sensitive Channels on the African Monsoon during AMMA

FATIMA KARBOU, FLORENCE RABIER, JEAN-PHILIPPE LAFORE, AND JEAN-LUC REDELSPERGER

CNRM-GAME, Météo-France and CNRS, Toulouse, France

OLIVIER BOCK

Laboratoire de Recherche en Géodésie/IGN, Marne La Vallée, France

(Manuscript received 10 December 2008, in final form 5 June 2009)

ABSTRACT

Observations from Advanced Microwave Sounding Unit-A and -B (AMSU-A and -B) have been more intensively used over sea than over land because of large uncertainties about the land surface emissivity and the skin temperature. Several methods based on a direct estimation of the land emissivity from satellite observations have been found to be very useful for improving the assimilation of sounding channels over land. Feasibility studies have been conducted within the Météo-France global assimilation system in order to examine the possibility of assimilating low-level atmospheric observations receiving a contribution from the land surface. The present study reports on three 2-month assimilation and forecast experiments, which include the assimilation of surface-sensitive observations from AMSU-A and -B together with a control experiment, which represents the operational model. The assimilation experiments have been compared with the control, and important changes in the analyzed atmospheric fields and in the precipitation forecasts over parts of the tropics, and especially over West Africa, have been noticed. The experiments seem to emphasize the atmospheric moistening in India, South America, and in West Africa, together with atmospheric drying over Saudi Arabia and northeast Africa. The drying or moistening of the atmosphere has been successfully evaluated using independent measurements from the GPS African Monsoon Multidisciplinary Analysis (AMMA) network. Precipitation and OLR forecasts have also been examined and compared with independent measurements. Physically, the changes result in a better-organized African monsoon with a stronger ITCZ in terms of ascent, vorticity, and precipitation, but there is no northward shift of the monsoon system. Low-level humidity observations have been found to have important impacts on the analysis and to produce positive impacts on forecast scores over the tropics.

1. Introduction

The West African monsoon (WAM) is still far from being well represented in numerical weather prediction (NWP) models. The WAM is governed by multiple mechanisms, which show very complex interactions that are not yet fully understood. Not surprisingly, a realistic representation of the spatial distribution, the strength, and the duration of the WAM remains a great challenge. The atmospheric water vapor is responsible for the cloud formation and plays a crucial role in convection and pre-

cipitation processes. A good description of the water vapor distribution (in space and in time) should be very helpful to better constrain the monsoon representation in NWP models in terms of spatial distribution and strength. Moreover, such achievements will help us to better understand the complex interactions involving the humidity fields during the different phases of the West African monsoon. Few in situ humidity observations are available over Africa. The African Monsoon Multidisciplinary Analysis (AMMA) research program (Redelsperger et al. 2006) was launched with the aim of enhancing our understanding of the West African monsoon. For a limited time period, the radiosonde network over West Africa became less sparse. However, even with additional radiosondes, the network is still far from

Corresponding author address: Fatima Karbou, CNRM-GAME, Météo-France and CNRS, 42 Av. Coriolis, 31057 Toulouse, France.
E-mail: fatima.karbou@meteo.fr

being optimal. Within the AMMA project, a small ground-based network of the global positioning system (GPS) has been developed over West Africa during the special observing period (SOP). GPS observations have been found very useful for measuring the precipitable water vapor (PWV) at different scales over Africa (Bock et al. 2007). The humidity measurement network has been temporally extended as part of AMMA, but more effort is still necessary in order to provide additional estimates of the humidity over all surfaces with good temporal and spatial sampling. Observations from satellite sensors such as the Advanced Microwave Sounding Unit-A and -B (AMSU-A and -B), which have considerable information content, gave a valuable description of the temperature and humidity at different levels in the atmosphere. The use of these measurements in NWP has led to substantial progress being made, but more effort is needed to assimilate many more observations in a wide range of atmospheric situations (clear, cloudy) and with a variety of surface conditions (ocean, land, snow, etc.). However, many issues are still to be addressed, in particular, the assimilation of observations in the presence of clouds and over land surfaces. The assimilation of cloud-affected Special Sensor Microwave Imager (SSM/I) observations has been operational at the European Centre for Medium-Range Weather Forecasts (ECMWF) since June 2005 (Bauer et al. 2006a,b). Significant headway was made possible when a two-step method [one- and four-dimensional variational data assimilation (1D + 4DVAR)] was adopted to assimilate a selection of cloudy, sea SSM/I observations. In parallel, studies have been carried out in order to improve the land surface emissivity modeling within the constraints of the Météo-France assimilation system and to help in assimilating more microwave observations over land and under clear-sky conditions (Karbou et al. 2006). It has been found that the use of an improved description of the land surface emissivity and/or skin temperature allows the assimilation system to take advantage of the information content of the AMSU temperature and humidity sounding channels over land (Karbou et al. 2010, hereafter Part I). These results are very encouraging and suggest that it is now possible to explore various strategies for assimilating surface-affected microwave observations. The purpose of this paper is to extend the use of satellite data to low-level atmospheric observations, which receive a contribution from the land surface. To test the ability of the Météo-France assimilation system to assimilate low-level humidity and temperature land observations from AMSU-A and -B, a comprehensive set of global 4DVAR assimilation and forecast experiments has been performed. In addition to the four 2-month experiments comprehensively described in Part I, three 2-month assimilation experiments were run for summer

2006. The first four experiments only differ in the land emissivity scheme used, and no additional AMSU-A and -B channels have been assimilated with respect to the control experiment. In the other three experiments, AMSU-A and -B observations, which are informative about the temperature and the humidity in the low levels of the atmosphere, have been assimilated for the first time over land. The impacts of assimilating such observations have been evaluated against a control experiment, which was the Météo-France operational system for July 2006. The results have also been evaluated against measurements from GPS stations over West Africa, outgoing longwave radiation (OLR) data from National Center for Atmospheric Research (NCAR), and against data from the Global Precipitation Climatology Project (GPCP). In this paper, the impacts of assimilating temperature and humidity observations over land are evaluated in terms of analysis and forecast skills with an emphasis on the impacts on the representation of the West African monsoon in the assimilation system. The experimental design is fully described in section 2. The impacts on the analyses and on forecasts are discussed in section 3, where data quality control issues are also discussed. In section 4, the humidity analysis is compared with estimates from GPS measurements over West Africa with a focus on the impacts on the WAM representation. In this section, rain and OLR forecasts are compared with precipitation estimates from GPCP and OLR data from NCAR, respectively. Conclusions are given in section 5.

2. Overview of experiments

This study is based on the Météo-France assimilation and forecast system (Action de Recherche Petite Echelle Grande Echelle, ARPEGE), which uses a 6-h time window and a multi-incremental 4DVAR scheme (Courtier et al. 1994; Veersé and Thépaut 1998; Rabier et al. 2000). The ARPEGE system was developed in collaboration with ECMWF. To describe the land surface emissivity at microwave frequencies, one method, out of three, has been chosen (called method 2 in Part I, but referred to as the dynamical method hereafter). This method uses dynamically varying emissivities derived at each pixel using observations from only one channel per instrument. The dynamically estimated emissivity is then assigned to the remaining channels. Emissivities dynamically derived at 50 GHz (AMSU-A channel 3) and at 89 GHz (AMSU-B channel 1) are assigned, respectively, to the remaining AMSU-A and -B channels. More details about the ARPEGE system's configuration, about the AMSU-A and -B observations, and about the methods of describing the land surface emissivities can be found in Part I. It is worth mentioning that the Météo-France

TABLE 1. Overview of the assimilation experiments. Conditions for use in the AMSU observations are presented in Table 2.

Expt	Surface description	AMSU channels used over land
CTL	Empirical models*	AMSU-A, channels 5–14 AMSU-B, channels 3 and 4
EXP4	Method 2	CTL + AMSU-B channels 2 and 5 over land
EXP5	Method 2	CTL + AMSU-B channels 2 and 5 over land and within $\pm 55^\circ$ of latitudes
EXP6	Method 2	CTL + AMSU-B channels 2 and 5, AMSU-A channel 4, and within $\pm 55^\circ$ of latitudes

* Empirical versions of Weng et al. (2001) and Grody et al. (1998).

assimilation system has been using the dynamical emissivity method operationally for land emissivity estimation at AMSU-A and -B frequencies since July 2008.

A set of four 2-month assimilation and forecast experiments are analyzed in this paper. The experiments have been run from 15 July to 14 September and have produced global analyses four times per day and 4-day forecasts every day at 0 h. For all the experiments, the initial conditions were taken from the operational analysis at 1800 UTC on 14 July 2006. The list of assimilation experiments is given in Table 1. Experiment CTL is our control experiment and is representative of the operational ARPEGE system. Three other experiments (called EXP4, EXP5, and EXP6) use the emissivity dynamical method to describe the land surface emissivity. Experiment EXP4 assimilates AMSU-B channels 2 and 5 observations over land. In EXP5, AMSU-B humidity observations from channels 2 and 5 are assimilated over land surfaces located within a $\pm 55^\circ$ latitude interval. Finally, EXP6 is identical to EXP5 but with the assimilation of observations from AMSU-A temperature channel 4 over land (within $\pm 55^\circ$ latitudes). The fundamental mo-

tivation for running EXP6 is to examine if the assimilation system is able to use the low-level temperature or humidity observations to improve the analysis and the forecast. The restriction of the assimilation to observations within $\pm 55^\circ$ latitudes is motivated by at least two reasons: (a) the need to identify areas where humidity observations can have the largest impact and (b) land emissivity biases (due to rain, snow, etc.) are more likely to occur over high-latitude areas. Such effects can potentially diminish the assimilation experiment's impacts. One should bear in mind that the observations from AMSU-B channels 2 and 5 and from AMSU-A channel 4 are normally either entirely rejected or assimilated over open sea only. Over land, additional conditions are applied to reject observations over high-altitude areas (greater than 1000 m) or if the departures from a first guess are greater than a fixed threshold. Table 2 summarizes the conditions for use of the AMSU observations in the system. Figure 1 shows the mean density maps of AMSU-B observations from channel 5, which have been assimilated during August 2006 in CTL (top panel) and in EXP4 (bottom panel), respectively. One should note

TABLE 2. AMSU-A and -B characteristics and conditions for use.

Instrument	Channel	Frequency (GHz)	Sensitivity	Conditions for use	Obs (FG) errors
AMSU-A	1	23.8	Surface	Not used	—
	2	31.4	Surface	Not used	—
	3	50.3	Surface	Not used	—
	4	52.8	Temperature	Used if land and mean orography <500 m	0.60 (0.70)
	5	53.596 ± 0.115	Temperature	Used if open sea, land, and mean orography <500 m	0.45 (0.54)
	6	54.4	Temperature	Used if open sea, land, and mean orography <1500 m	0.35 (0.21)
	7	54.9	Temperature	Not used if cloudy, $ \text{lat} \leq 30^\circ$	0.35 (0.17)
	8	55.5	Temperature	Not used if cloudy, $ \text{lat} \leq 30^\circ$	0.35 (0.20)
	9	$\nu = 57.290$	Temperature	Used	0.35 (0.23)
	10	$\nu \pm 0.217$	Temperature	Used	0.35 (0.23)
	11	$\nu \pm 0.322 \pm 0.048$	Temperature	Used	0.50 (0.31)
	12	$\nu \pm 0.322 \pm 0.022$	Temperature	Used	0.80 (0.41)
	13	$\nu \pm 0.322 \pm 0.010$	Temperature	Used	1.2 (0.64)
	14	$\nu \pm 0.322 \pm 0.0045$	Temperature	Not used	—
AMSU-B	15	89	Surface	Not used	—
	1	89	Surface	Not used	—
	2	150	Surface	Used if land and mean orography <500 m	2.00 (3.97)
	3	183 ± 1	Humidity	Used if open sea, land, and mean orography <1500 m	3.00 (2.63)
	4	183 ± 3	Humidity	Used if open sea, land, and mean orography <1000 m	2.50 (2.28)
5	183 ± 7	Humidity	Used if open sea, land, and mean orography <1000 m	2.00 (2.12)	

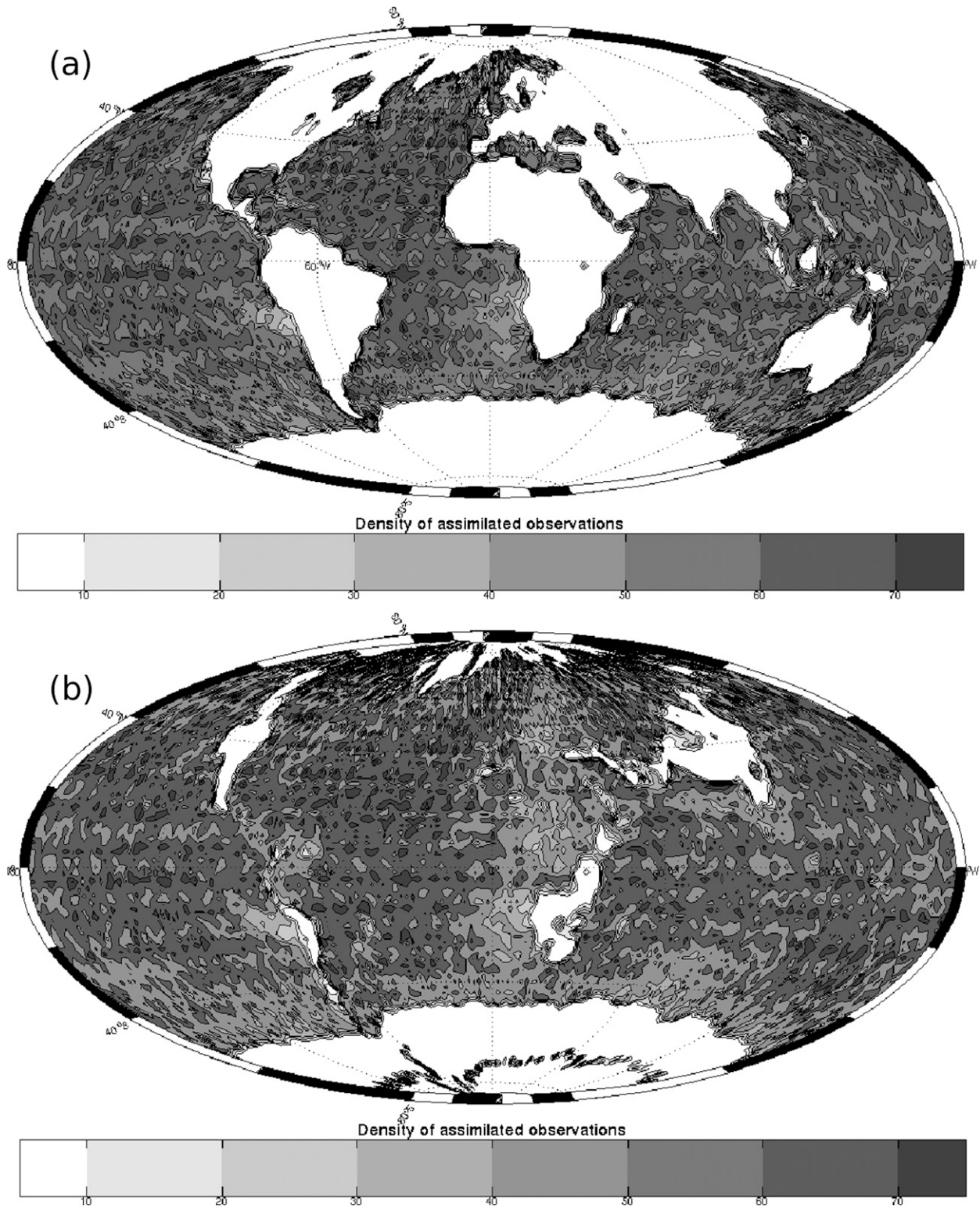


FIG. 1. (a) Map of the density of assimilated observations from AMSU-B channel 5 in the control experiment. The density values have been computed by counting the numbers of assimilated observations falling into a grid cell of $2^\circ \times 2^\circ$ size and during the month of August 2006. (b) As in (a), but for EXP4.

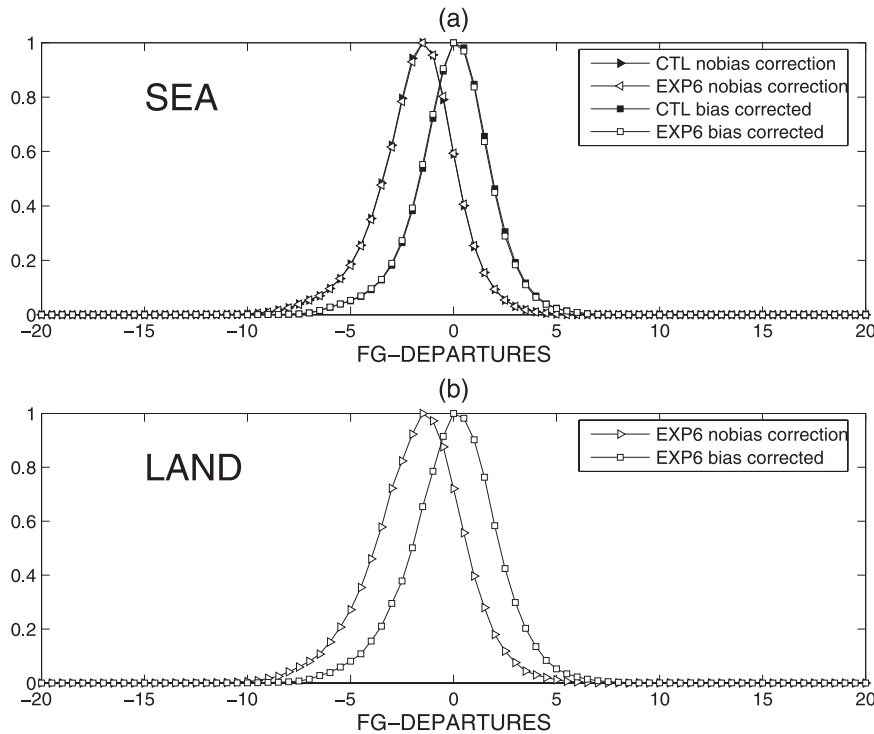


FIG. 2. FG departures (observations – simulations) of AMSU-B channel 5 computed for a 1-month period (August 2006) and for the CTL (curves with filled symbols) and EXP6 (curves with open symbols) experiments. Results are given with (curves with squares) and without (curves with triangles) the bias correction: (top) sea and (bottom) land.

the rather large increase in assimilated observations over land surfaces.

3. Impacts on analysis and forecasts

a. On data quality control and model fit to observations

As stated earlier, a significant number of observations over land have been assimilated in EXP4, as compared with the CTL experiment. To evaluate the performances of the observation operator over land and over sea, the differences between observed and simulated radiances using the background fields have been computed. The first-guess (FG) departures have been computed with and without bias correction. Global statistics for the August 2006 FG departures for assimilated AMSU-B channel 5 are presented in Fig. 2. The results are for CTL and EXP6. Land observations are separated from sea observations. One may note that the FG departure statistics are as good for EXP4 (sea and land observations) as they are for CTL (sea observations only) and that the bias correction over land successfully reduces the bias, as it does over sea. Similar results have been observed when analyzing FG departures from EXP5 and EXP6.

These findings also suggest that the surface channel FG departures are as good over land as they are over sea. The data quality controls (QC hereafter) are key elements for the successful assimilation of temperature and humidity observations. QC tests are generally used to reject data with a too strong cloud contamination. For AMSU observations, the QC tests are performed using FG departures from AMSU-A channel 4 (noted AMA4 hereafter) and AMSU-B channel 2 (noted AMB2 hereafter): AMB2 FG departures should be within ± 5 K and the AMA4 FG departures should be within ± 0.7 K. So far, many observations over land have been incorrectly rejected in CTL not because of cloud contamination but because the values for the land surface emissivity or of the skin temperature are inappropriate. However, the advantage of this setup is the fact that the channels used for QC testing are, in a way, independent from the assimilation, as they are not actively assimilated. In the new configuration, a feedback process could happen when assimilating a channel used for cloud screening. If this effect occurs, then the experiments could slowly drift. To check this, time series of the number of AMB2 and AMA4 observations for which the QC test was successful have been examined for all experiments. Figures 3 and 4 compare the obtained time series from CTL (dashed line)

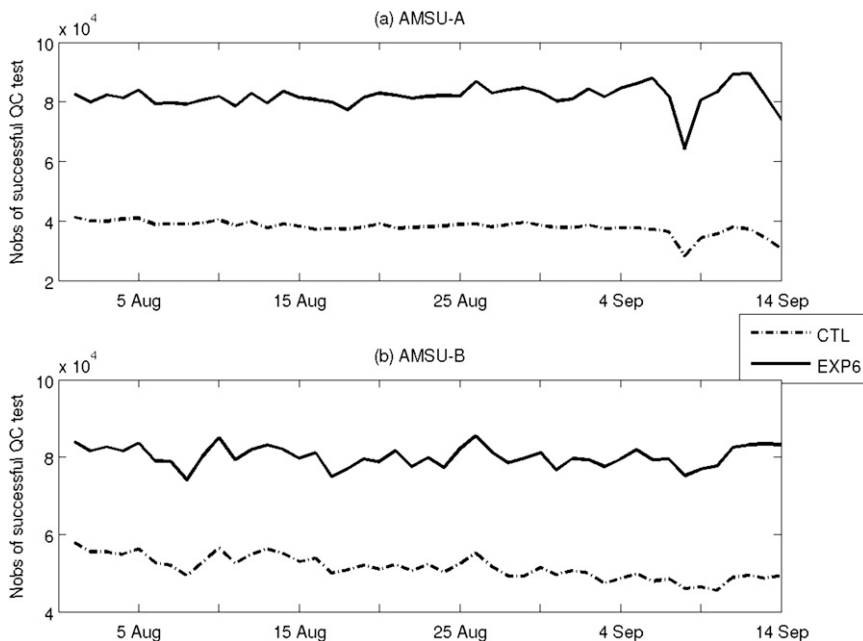


FIG. 3. (a) Time series of the total number of AMSU-A channel 4 observations for which the QC test in CTL (dashed line) and in EXP6 (solid line) was successful over land. (b) As in (a), but for AMSU-B channel 2.

and from EXP6 (solid line) using observations over land only and over all surfaces, respectively. AMB2 and AMA4 are not assimilated in the CTL, whereas they are both assimilated in EXP6. One can notice a general decrease

of the amount of successful QC data during August and its increase in September but no systematic trend can be observed for EXP6 with respect to CTL. In particular, no significant change over the ocean has been noted

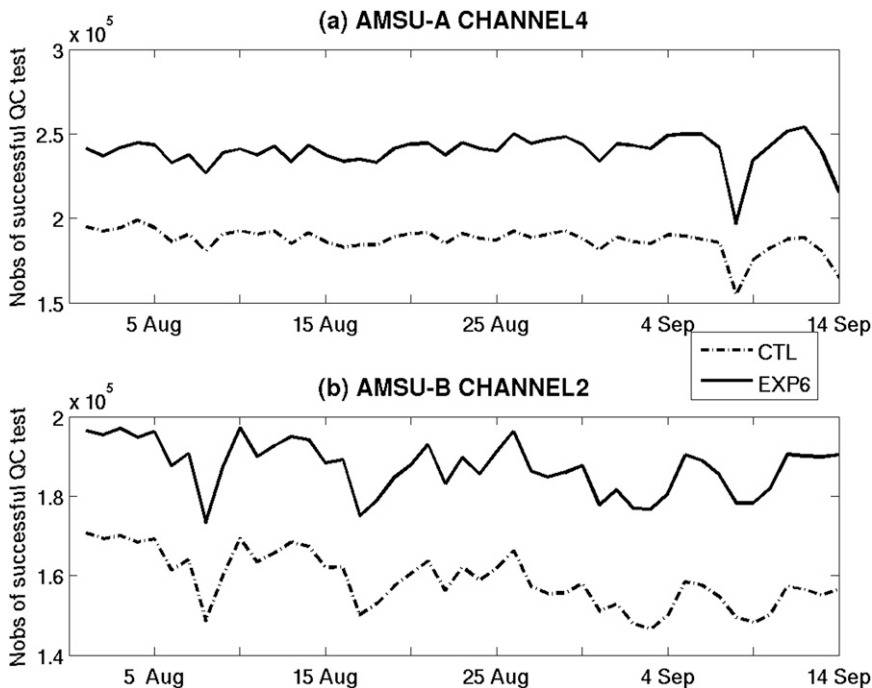


FIG. 4. As in Fig. 3, but for land and sea observations.

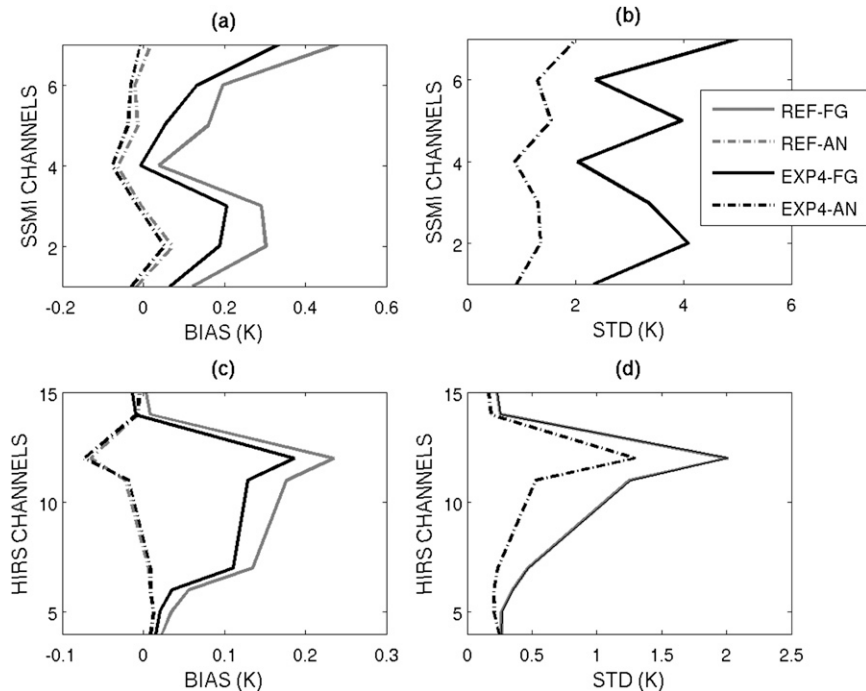


FIG. 5. (a) Bias and (b) standard deviation for the FG (solid) and for the analysis departures (dashed) for assimilated SSM/I observations for EXP4 (black) and CTL (gray). (c),(d) As in (a),(b), but for HIRS observations. The period is August 2006.

between EXP6 and CTL. The QC controls seem to be working better when the land surface emissivity is better described.

The general findings about the model fit to the observations are that there is no divergence between the assimilation of surface-sensitive observations over land and the assimilation of other observations. Indeed, the fit of other observations against FGs or analyses is not altered when surface-sensitive temperature or humidity observations are assimilated over land. The fit of the SSM/I and High Resolution Infrared Radiation Sounder (HIRS) observations compared to that the FG is even better than in CTL for EXP4–EXP6, especially over the tropics. These observations are very informative about the humidity in the atmosphere. Figure 5 shows the model fit in terms of bias and standard deviation (panels a and b, respectively) to SSM/I and to HIRS observations (panels c and d, respectively) over tropical regions (within $\pm 20^\circ$). For SSM/I, the FG bias for EXP4 (black) is significantly smaller than in CTL (gray) with approximately the same number of assimilated SSM/I observations. Similar conclusions can be drawn when looking at the results for the HIRS observations. These results imply that EXP4 (and by the same token, EXP5 and EXP6; not shown) successfully brings the simulations of the humidity measurements closer to the observations.

b. The forecast impact

The forecast impacts has been studied by examining the short-range verification scores of precipitation and OLR at 24-h range and longer-range verification scores (up to 4 days) for mass, wind, relative humidity, and temperature fields. For each parameter, the forecast root-mean-square errors (RMSEs) have been calculated for August 2006; for all experiments, the radiosonde observations or verifying analyses from ECMWF were the target estimations. Figure 6 shows the differences in bias and RMSE between the 48-h forecast of geopotential for EXP6 (black) and CTL (gray) with respect to the radiosonde observations. The results are for four regions: the Northern Hemisphere, Australia–New Zealand, the Southern Hemisphere, and the tropics. General improvement in the bias in EXP6 can be noticed for all domains and at many pressure levels. The best results are obtained in the tropics and over Australia–New Zealand, where the density of the radiosondes is satisfactory. The reduction in forecast errors over the tropics is statistically significant at the 90% confidence level or better (Student's *t* test). Figure 7 shows time series of temperature forecast errors in the tropics at 250 hPa (bias and RMSE) with respect to the ECMWF analyses. Results are for CTL (gray), EXP6 (black), and for four forecast ranges:

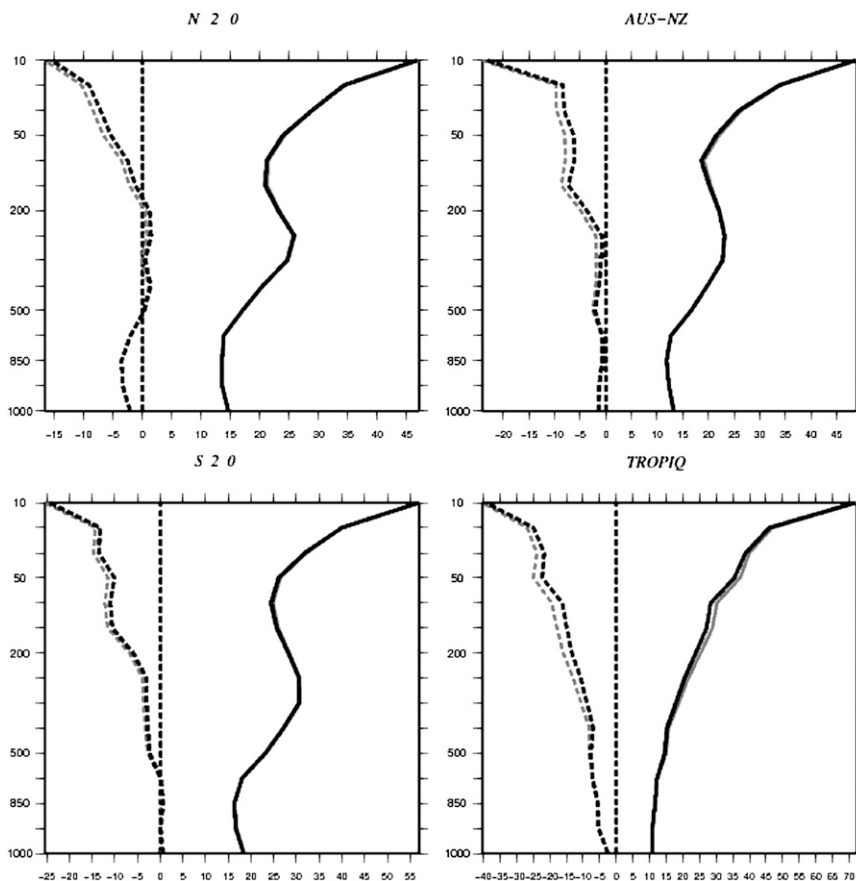


FIG. 6. RMSE (solid lines) and mean bias (dashed lines) for geopotential differences between the 48-h forecasts of CTL (gray) and EXP6 (black), with the radiosonde providing the target observations. Results are given for (top left) the Northern Hemisphere, (top right) Australia–New Zealand, (bottom left) the Southern Hemisphere, and (bottom right) the tropics.

24, 48, 72, and 96 h. A systematic decrease in the temperature bias can be observed for EXP6 at all forecast ranges. The effects on temperature are statistically significant, are observed at many pressure levels, and suggest that EXP6 is significantly better than CTL in the tropics. Similar results have been obtained with geopotential forecast scores for EXP5 and EXP6. To pursue these investigations, the differences in geopotential scores (CTL-EXP4) with respect to ECMWF analyses have been calculated for August 2006. Results for 200 hPa and forecast ranges (a) 24, (b) 48, and (c) 72 h are presented in Fig. 8. Red colors indicate that the forecast errors in CTL are larger than the forecast errors in EXP4. Geopotential errors are reduced in EXP4 over large parts of Africa and this improvement propagates at 48 and 72 h to higher latitudes. The geopotential forecast improvement with respect to ECMWF analyses is statistically significant at the 90% confidence level at 24 h and at the 95% confidence level at 48 and 72 h (Student's *t* and bootstrap tests). The EXP4 forecast scores are

slightly better than those of EXP5 and EXP6. The forecast impacts have also been examined by analyzing the short-range forecasts of precipitation and OLR. The results will be fully discussed in the next section.

4. On the representation of the West African monsoon

When assimilating near-surface microwave observations, the largest impacts on the analyses and forecasts occur over tropical regions. For this reason, we will focus, in the following, on the changes to the analysis of atmospheric fields and on the changes to the precipitation and OLR forecasts over parts of the tropics and especially over West Africa.

a. Evaluation of TCWV with GPS measurements

Figure 9a shows the mean analysis difference in TCWV between EXP5 and CTL averaged over 45 days (1 August–14 September 2006) and Fig. 9b shows the corresponding

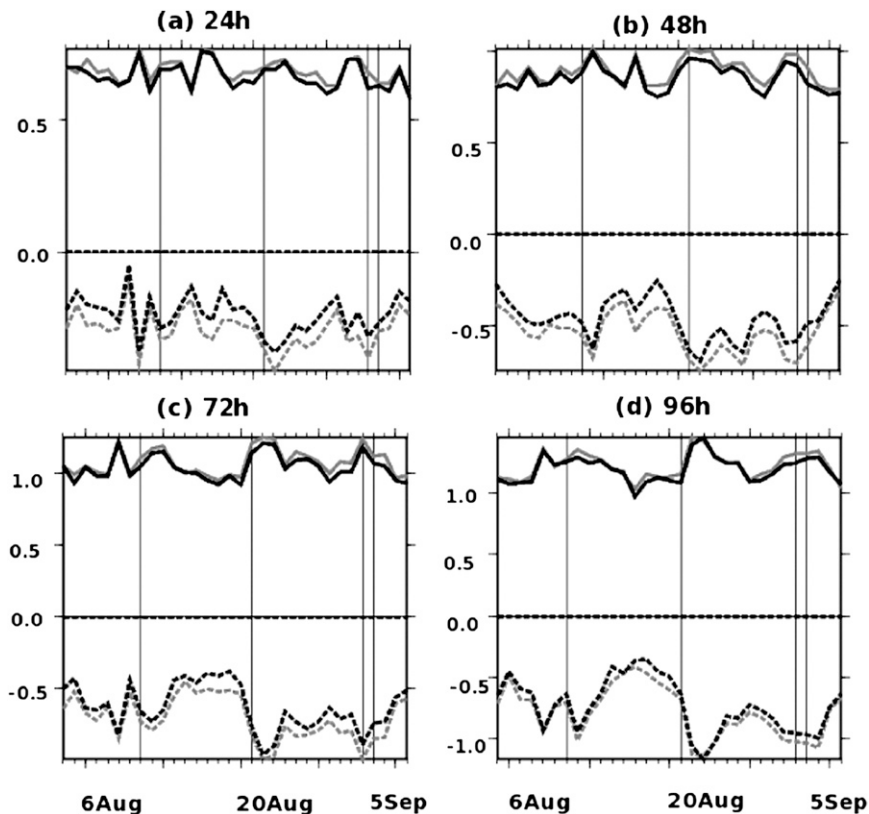


FIG. 7. Time series of RMSE (solid lines) and mean bias (dashed lines) for temperature differences in the tropics at 250 hPa between the CTL (gray) and EXP6 (black) forecasts, with the verifying ECMWF analyses being the target. Results are for (a) 24-, (b) 48-, (c) 72-, and (d) 96-h forecasts.

average of TCWV from CTL. When the TCWV differences are positive (negative), EXP5 is moister (drier) than CTL. One may notice the drying and moistening features over the land surfaces. EXP5 at least for the Northern Hemisphere seems to emphasize the moistening over India, South America, and in western and central Africa in monsoon regions. On the other hand, EXP5 also emphasizes drying over Saudi Arabia and over the desert regions of northeast Africa. The drying or moistening of the atmosphere is far from being negligible (cf. the maps in Figs. 9a and 9b for the relative changes in TCWV), reaching +10% and 20% over wet and desert regions, respectively. The results from EXP4 and EXP6 are quite similar to those of EXP5, suggesting that the effects of the low-level AMSU-B observations over land are dominant. Such impacts can be essential for the WAM system as it strengthens the humidity dipole over West Africa and can also be important for the location of the intertropical convergence zone (ITCZ) and of the intertropical discontinuity (ITD).

However, how realistic is the increase or the decrease of TCWV over land when assimilating low-level hu-

midity data? Ideally, the analyzed TCWV should be compared with independent TCWV measurements. Six GPS stations operating over West Africa during August 2006 were used as target measurements to evaluate the analyses of TCWV (see Fig. 10 for the geographic locations of the stations). TCWV time series from GPS measurements are a good indicator when evaluating the TCWV variability tendency in our analyses. The comparison has been made using 45 days of GPS measurements. For each experiment and for each GPS station, the four closest grid points to the GPS station have been determined to calculate an averaged TCWV from the analyses. Table 3 shows TCWV statistics (mean, standard deviation) from GPS and from all of the 4DVAR experiments. For the assimilation experiments, the statistics included all analysis cycles (0000, 0600, 1200, and 1800 UTC). For GPS, the statistics included measurements at the same times. Correlations between TCWV from GPS and CTL are presented in Table 4 together with correlation differences (EXP - CTL, EXP correlations with respect to GPS). The results show that the comparison with GPS measurements is in favor of experiments

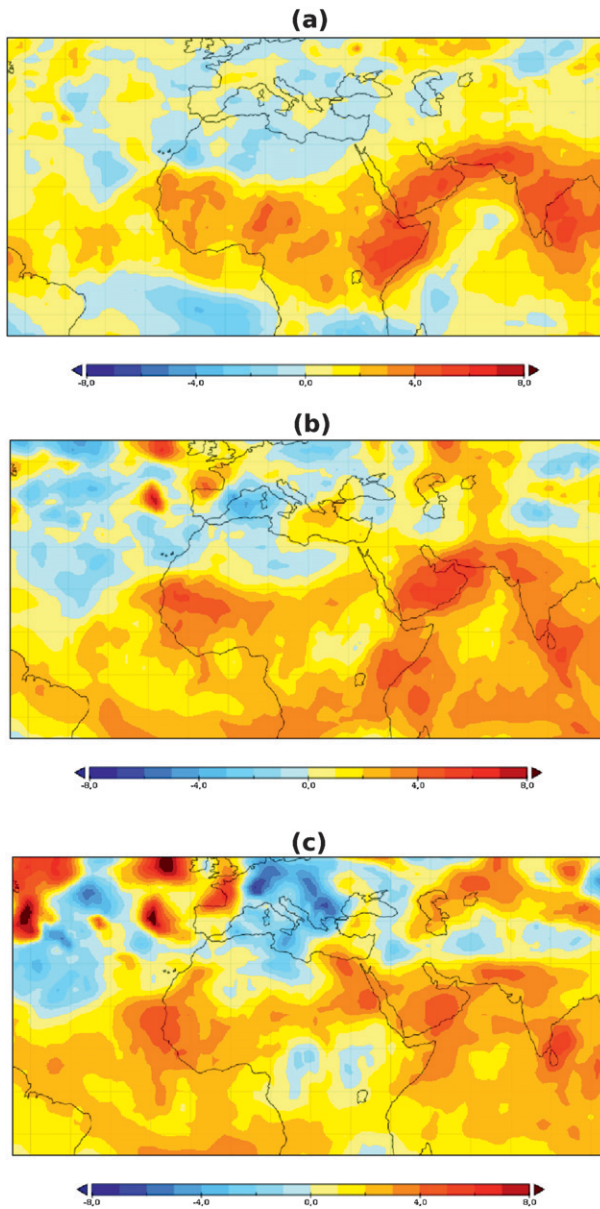


FIG. 8. Differences in RMS error between the CTL and EXP4 forecasts (CTL – EXP4) at the (a) 24-, (b) 48-, and (c) 72-h range. Errors are computed for August for 200-hPa geopotential height with respect to the ECMWF analyses.

assimilating low-level microwave observations. For the mean bias, the improvement is clear for Timbuktu, Mali (TIMB), and Ouagadougou, Burkina Faso (OUAG), sampling the moistening region by the assimilation in terms of $\delta TCWV$ (see Fig. 9a). The correlations are also systematically higher for these experiments than for CTL (up to +0.07 improvement for Timbuktu and +0.04 for Ouagadougou). Figure 11 compares the mean correlation values per GPS station computed using 45 days of data (all synoptic times) from CTL and EXP4–EXP6

with respect to the GPS measurements. The correlation is improved for all stations and the EXP4 results are comparable to those of EXP5 and EXP6. The correlation improvement is statistically significant for all stations. This means that the TCWV variability is better represented when low-level humidity observations are assimilated over land. To illustrate this, Fig. 12 compares mean daily TCWV time series at Ouagadougou computed from the GPS measurements (gray line) and from analyses of CTL and EXP4–EXP6. The image shows how close the TCWVs from the experiments (EXP4–EXP6) are to ground-based measurements, which is in contrast to CTL. The results at Timbuktu have been further studied in Fig. 13 to analyze the TCWV mean diurnal cycle. Contrary to CTL (flat), EXP4 recovers a realistic diurnal cycle both in phase and magnitude as compared with the GPS estimates. This may explain why TCWV standard deviations from EXP4 are slightly larger than those from CTL. The mean bias is also improved, in agreement with Table 3. Mean TCWV analyses from EXP4–EXP6 have been found to be statistically closer to the GPS estimates for Gao, Mali (GAO1); Djougou, Benin (DJOU); and Tamale, Ghana (TAMA), at 5% confidence level.

b. Effect of near-surface observations

This section examines the importance of assimilating low-level temperature and humidity observations for the analysis and for the forecast, and to what extent it could be linked to the WAM representation in the model. As stated earlier, the largest impact is observed in the tropics. The assimilation of near-surface observations leads to important drying–moistening coherent structures over parts of the tropics, including West Africa. The humidity change not only concerns low levels but also midlevels (up to 500 hPa). Figures 14a and 14b show mean maps of analysis differences for temperature (δT) and for specific humidity (δq) at 950 hPa. The results are for EXP5 with respect to CTL. As expected, all zones exhibiting positive (negative) $\delta TCWV$ corresponds to moistening (drying) zones at the surface after comparison with Fig. 9a. Nevertheless, the structures at the surface are less extended than for $\delta TCWV$. For temperature, the assimilation behaves in an opposite way, with cooling at the surface in zones exhibiting positive $\delta TCWV$ and moistening at the surface. Nevertheless there is no warming in dry zones. The cooling spots occur over South America, India, and Africa, but are much stronger over western and central Africa (-2.5 K). This could be the result of the limited observation network over Africa, except in the vicinity of the Greenwich longitude, where the radiosonde network has been largely improved during AMMA. The baroclinicity at low levels

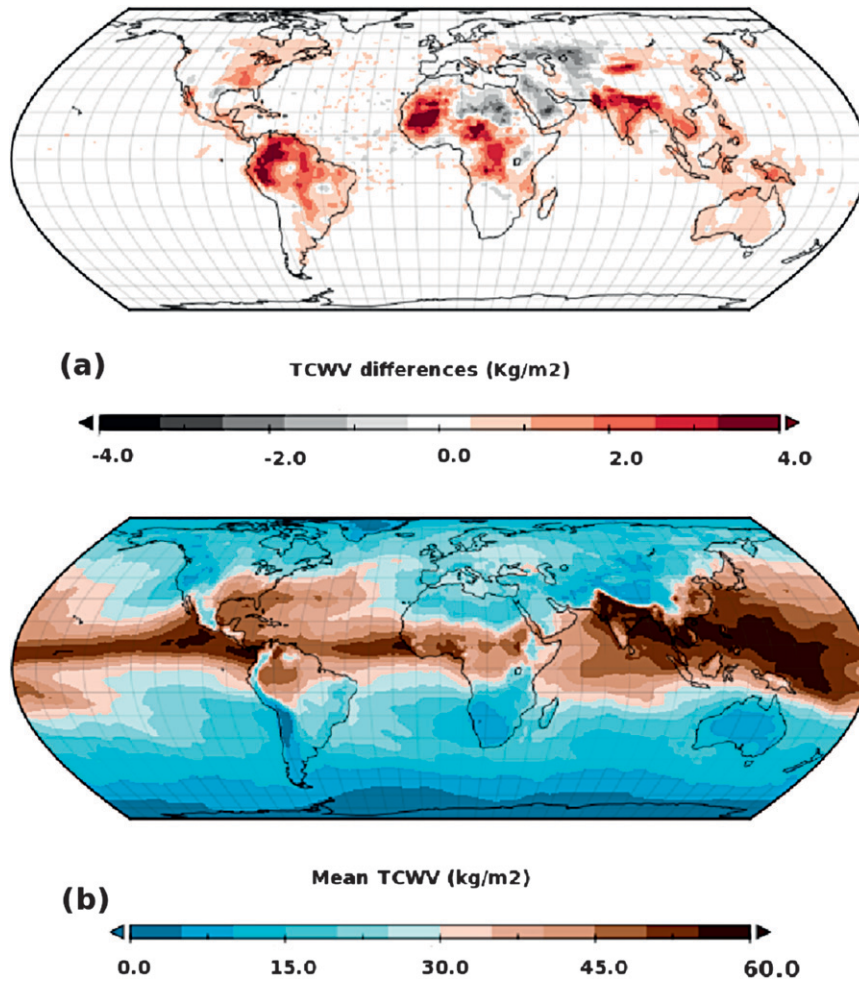


FIG. 9. (a) Mean analysis difference for TCWV for the EXP5 experiment with respect to the control. Statistics have been derived using 45 days (1 Aug–14 Sep 2006). Negative (positive) values indicate that the control assimilation is moister (drier) than in the EXP5 experiment. (b) Mean analysis for TCWV for the control experiment averaged over 45 days.

changes as well over Africa due to the assimilation of low-level microwave observations. The pattern can explain the significant change in the zonal wind (δV_z) at 700 hPa (up to 2.5 m s^{-1}) in regions where the baroclinicity changes, especially in central Africa (Fig. 14c).

The results from EXP5 and EXP6 (not shown) are similar to those of EXP4, which indicate that low-level humidity observations from AMSU-B have the largest impacts in the analysis. To analyze the vertical structure of the impacts of the assimilation of AMSU-B, we selected a mean latitude–height cross section, averaged over $10^\circ\text{--}20^\circ\text{E}$ (Fig. 15). The moistening (δq ; 0.5 g kg^{-1} on average) spreads throughout the atmosphere up to 500 hPa between 10°S and 18°N . Its maximum is at the surface (1.7 g kg^{-1}) at 14°N (Fig. 15a). The moistening is associated with a systematic cooling of the atmosphere up to an 800-hPa maximum at the surface (-2 K), un-

derneath a weak warming ($+0.3 \text{ K}$) layer at 600 hPa (Fig. 15b). The vertical stability consequently increases in the monsoon region south of 20°N . The meridional baroclinicity strongly increases north to 15°N and

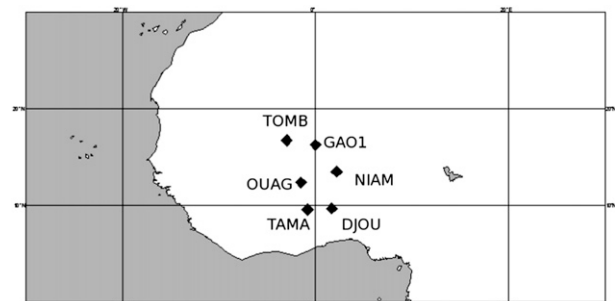


FIG. 10. AMMA GPS stations over West Africa used in this study.

TABLE 3. TCWV statistics (means, standard deviations in kg m^{-2}): analyzed TCWVs in CTL (in bold) and EXP4–EXP6 are compared with GPS estimates at six stations. Statistics are for 45 days (1 Aug–14 Sep 2006) and at four synoptic times (0000, 0600, 1200, and 1800 UTC).

GPS station		GPS	CTL-GPS	EXP4-GPS	EXP5-GPS	EXP6-GPS
TIMB	Mean	41.71	-2.74	0.99	0.54	0.72
	Std dev	5.85	0.58	1.73	1.56	1.10
NIAM	Mean	47.09	0.11	0.78	0.51	0.54
	Std dev	5.15	-0.60	-0.27	-0.25	-0.26
OUAG	Mean	47.63	-1.74	0.15	0.09	-0.24
	Std dev	4.44	0.12	0.46	0.43	0.36
GAO1	Mean	41.16	1.02	3.39	3.46	3.29
	Std dev	5.86	-0.38	0.45	0.01	-0.01
TAMA	Mean	50.04	0.80	1.01	0.93	0.89
	Std dev	3.96	-0.14	0.02	-0.09	-0.02
DJOU	Mean	46.89	2.71	2.66	2.57	2.57
	Std dev	3.96	-0.50	-0.34	-0.36	-0.33

decreases south 15°N . The change in zonal wind (δV_z) directly depends on the previously mentioned change in baroclinicity (Fig. 15c) apparently due to the geostrophic balance, with positive ($+2.2 \text{ m s}^{-1}$) and negative (-1 m s^{-1}) changes at 750 hPa at 6° and 12°N , respectively. The AEJ thus is reinforced, with an increase in the positive vorticity on its southern flank. All of these changes in intensity and width of the AEJ in the Sudan region may change the activity of African easterly waves (AEWs) downstream in response to the convection activity coupled with AEWs (Leroux and Hall 2009). At this same level and at the same location of vorticity increase, Fig. 15d shows a large dipole of meridional wind change corresponding to a large convergence zone ($+1$ and -0.7 m s^{-1}). This results in a significant intensification of the deep ascent in the ITCZ (8°N) (0.5 cm s^{-1}) and a widespread reduction, in particular at the ITD (21°N). We should note also an intensification of the reverse flow at 750 hPa above the monsoon flux between the ITD and the ITCZ (Zhang et al. 2006). All these changes for all variables due to the assimilation of low-level microwave observations are coherent and correspond at this location (central Africa) to a better-organized active monsoon. The moistening does not result in a northward shift of the monsoon due to stabilization effects.

TABLE 4. Correlations between TCWV estimates from GPS stations and TCWVs analyzed in CTL and the correlation differences between EXP4–EXP6 and CTL (EXP – CTL). Statistics are for 45 days (1 Aug–14 Sep 2006) and for all assimilation cycles (0000, 0600, 1200, and 1800 UTC).

GPS station	CTL	EXP4 – CTL	EXP5 – CTL	EXP6 – CTL
TIMB	0.726	0.066	0.058	0.056
NIAM	0.841	0.020	0.016	0.013
OUAG	0.676	0.021	0.040	0.031
GAO1	0.696	0.018	0.026	0.001
TAMA	0.741	0.013	0.004	0.004
DJOU	0.593	0.035	0.036	0.039

We now analyze the impacts of the assimilation of low-level microwave observations on the precipitation forecast. Figure 16 shows the average of the 24-h cumulated rain forecast differences showing EXP5 minus CTL. Statistics are for 45 days. A global decrease of precipitation over tropical oceans (especially the eastern Atlantic) and an increase over continents has been observed. This pattern reduces a well-known deficiency in most models. The relative magnitude of these changes is significant (10%). For West Africa, we note a strong increase over Guinea and a decrease over Ghana and Togo, corresponding to an improvement. The precipitation increase is limited to south of 15°N . For South America, we note a strong increase over the northeast region that is also coupled with an increase in the regional convergent and cyclonic circulation at low levels (not shown), feeding convection. For the Indian monsoon, precipitation increase significantly over the Gulf

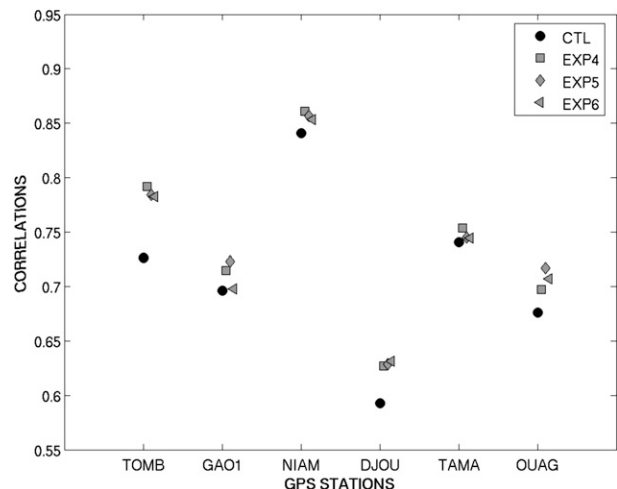


FIG. 11. Mean TCWV correlations between GPS and the analyses of CTL and EXP4–EXP6. Results are for six GPS stations and for 45 days (including all synoptic times).

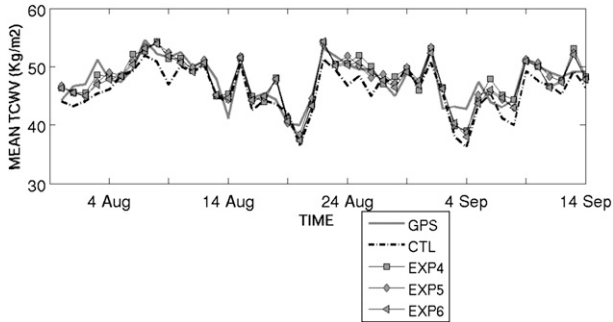


FIG. 12. Daily mean estimates of TCWV using GPS at OUAG station and daily mean TCWV analysis from CTL and EXP4–EXP6. Results are for a 45-day period (1 Aug–14 Sep 2006, including all synoptic times).

of Bengal and the Oman Sea. Figures 17a–c, respectively, show the precipitation estimates from GPCP, and the total first 24 h of precipitation from CTL and from EXP5 for August 2006. The comparison of GPCP precipitation and rain forecasts shows EXP5 to be best: 1) a rainfall maximum close to the Guinea Gulf is better represented in EXP5 than in CTL, 2) a lack of precipitation below 15°N is observed in CTL and seems to be corrected in EXP6, and 3) a rain increase is observed over South America and seems to be in good agreement with GPCP. Figure 18 shows the time evolution of the mean rain rate as a function of the forecast range for all four experiments. Results are given in Fig. 18a for the globe and in Fig. 18b for the tropics. The assimilation of

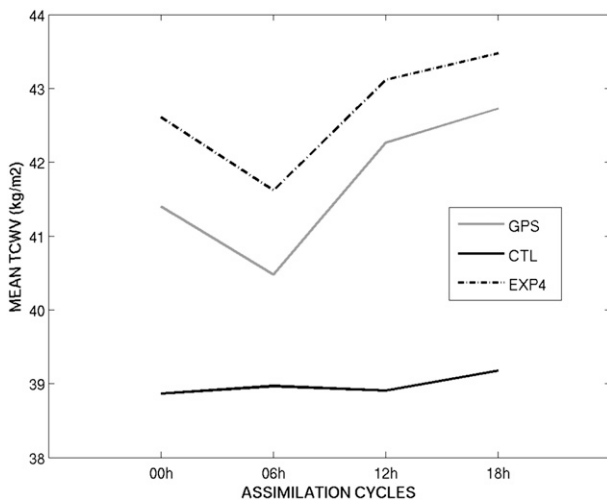


FIG. 13. Mean estimates of TCWV obtained from measurements at the TIMB GPS station, and the mean analysis near TIMB for TCWV for the CTL (black solid curve) and for EXP4 (black dashed curve) at 0000, 0600, 1200, and 1800 UTC. At each cycle, the TCWV mean values were averaged over a 45-day period (1 Aug–14 Sep 2006).

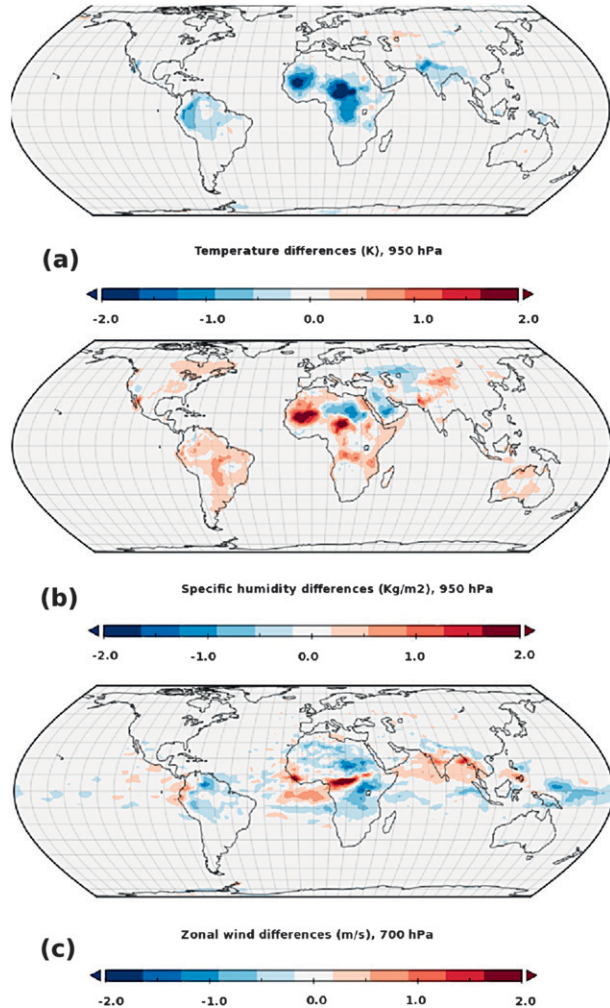


FIG. 14. (a) Mean difference map between the temperature analyses at 950 hPa from the CTL and the EXP5 experiments. Results are given for a 45-day period including analyses at 0-, 6-, 12-, and 18-h cycles. (b) As in (a), but for specific humidity. (c) As in (a), but for the zonal wind at 700 hPa.

low-level microwave observations successfully adds humidity in key areas in the tropics, increasing the precipitation; however, “spindown” problems are likely to occur as this impact is lost after 1 day, the model going back to its own equilibrium. Such a problem cannot be solved unless deeper changes are made to the moist physics parameterization to improve the model equilibrium and to bring it closer to the observations. In addition to precipitation forecasts, the total first 24 h of OLR have been computed from CTL and from EXP5, and have been compared with independent OLR estimates from NCAR (Liebmann and Smith 1996). OLR estimates can give good insights into deep tropical convection areas and high cloud distribution. Figures 19a–c show, respectively, the mean NCAR OLR estimates (denoted OLR-CLIM

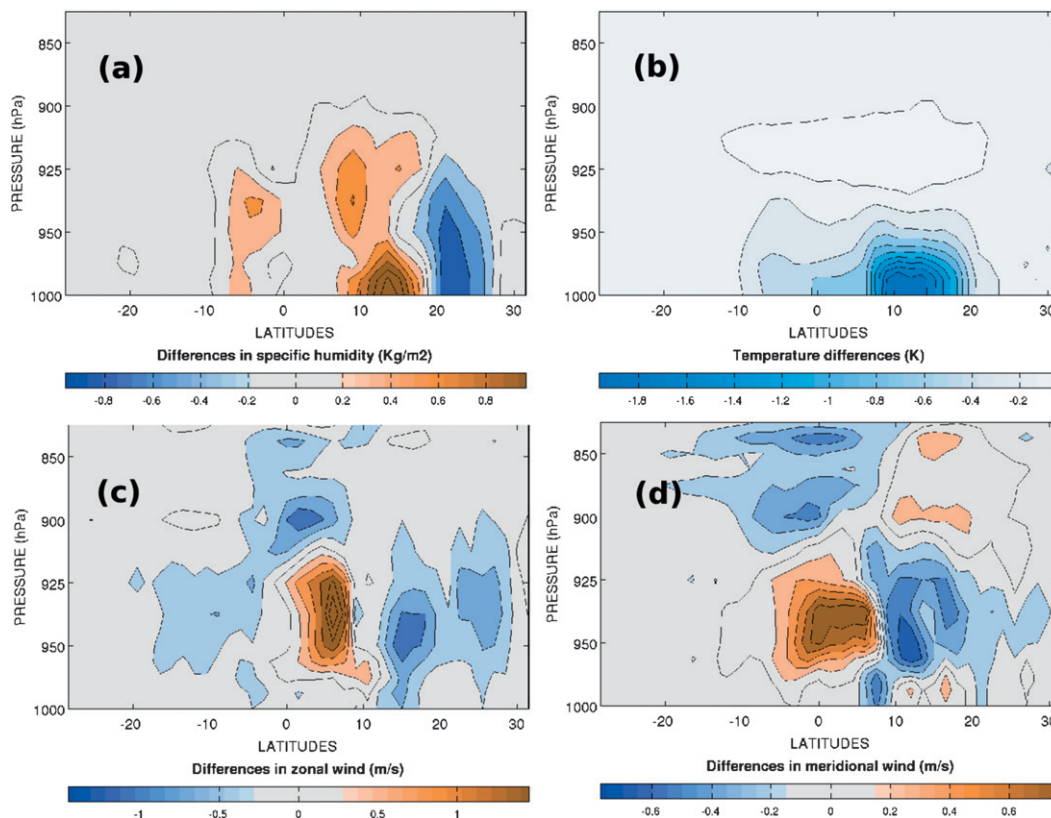


FIG. 15. (a) Latitude–pressure level cross section of the specific humidity differences (kg m^{-2}) along 10° – 20° E between the analyses of EXP5 and CTL over 45 days (1 Aug–14 Sep 2006), including analyses at 0-, 6-, 12-, and 18-h cycles. (b) As in (a), but for the temperature (K). (c) As in (a), but for the zonal wind (m s^{-1}). (d) As in (a), but for the meridional wind (m s^{-1}).

hereafter) for August 2006, the $\text{OLR}(\text{CTL}) - \text{OLR-CLIM}$, and the $\text{OLR}(\text{EXP5}) - \text{OLR-CLIM}$. Even though biases persist between the OLR-CLIM and OLR forecasts, the EXP5 OLR forecasts are closer to OLR-CLIM over West Africa. The OLR change in EXP5 partly reflects the change in analysis and forecasts of humidity and seems to be in good agreement with independent OLR measurements.

5. Concluding remarks

Several global assimilation and forecast experiments have been run in order to investigate the usefulness of the assimilation of surface-sensitive observations over land. The assimilation of such observations was made possible after alternative methods for estimating the land surface emissivity and the skin temperature were

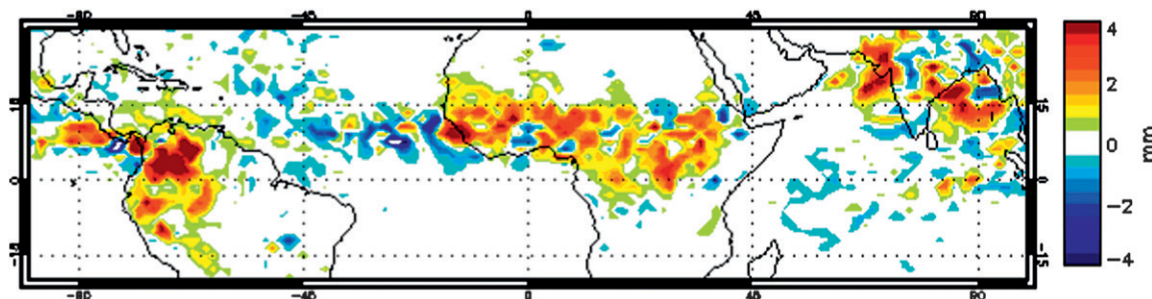


FIG. 16. Average of the 24-h forecast cumulative rain-rate difference over 45 days (1 Aug–14 Sep 2006) showing EXP5 – CTL. Positive (negative) values indicate that EXP5 has increased (decreased) the precipitation.

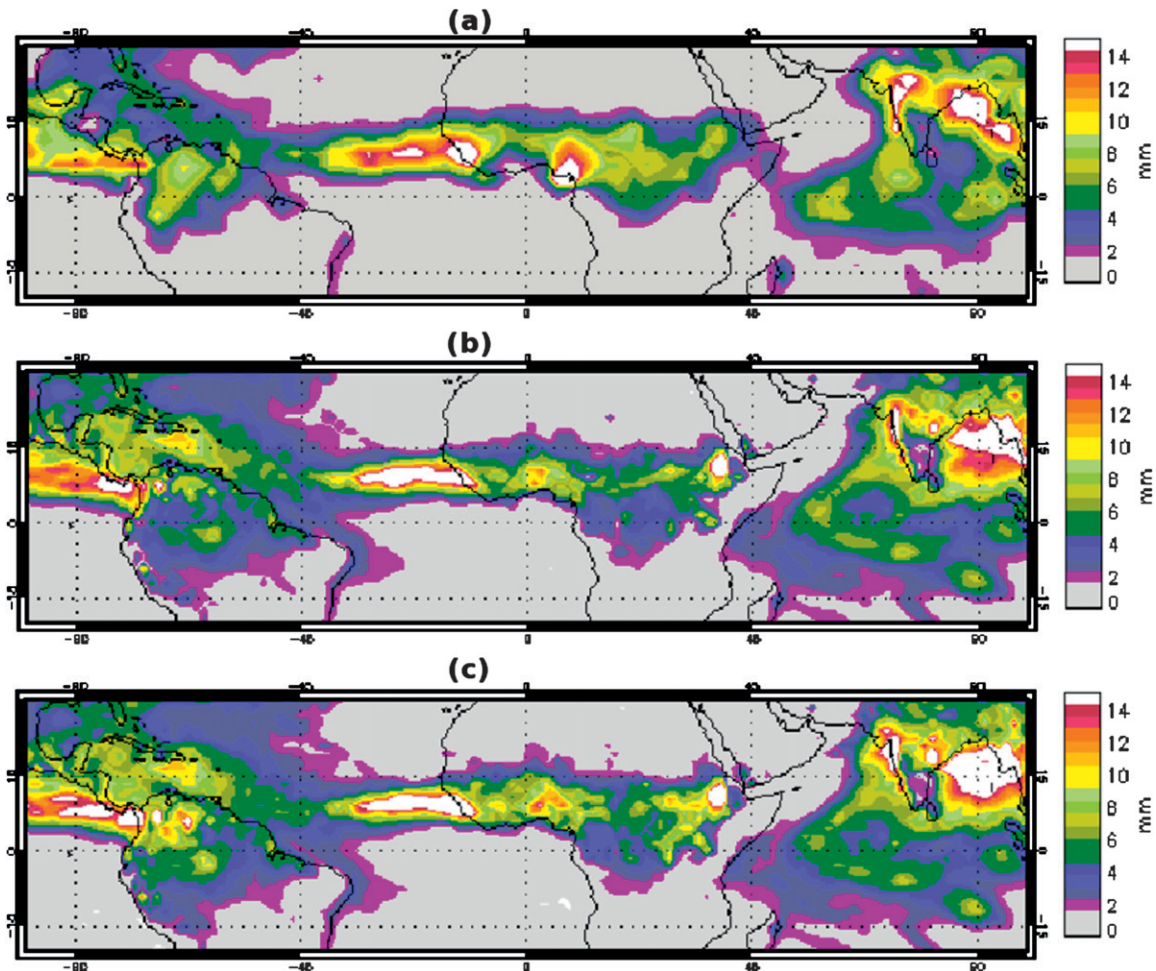


FIG. 17. (a) Main precipitation estimates from GPCP during August 2006 and (b),(c) the average of the 24-h accumulated rain rate using forecasts from (b) CTL (c) and EXP5.

developed in the Météo-France data assimilation system. The impacts of assimilating surface-sensitive observations from AMSU-A and -B over land have been studied with respect to a control experiment, which was representative of the operational model. Adding significantly more microwave data over land did not alter the model fit to all of the observations. The model fit to the observations has been significantly improved for SSM/I and HIRS observations mainly in the tropics. The study also revealed that the use of a new land surface emissivity scheme is beneficial for increasing the number of assimilated observations not only from surface-sensitive channels but also from sounding channels. The increase in assimilated observations has not been found to be harmful to the data quality controls. When comparing our set of experiments with respect to the control, the forecast scores against radiosondes have been found to be positive in the tropics and neutral elsewhere. The forecast scores with respect to ECMWF analyses have

been found to be positive for geopotential and temperature for forecast ranges up to 72 h. These results are very encouraging and suggest that it is possible to take advantage of the information content of the surface-sensitive observations over land if an adequate modeling of the emissivity and/or skin temperature is introduced. The key finding of this paper is that the largest impacts on the analyses and forecasts when assimilating near-surface microwave observations occur over tropical regions. The changes in the atmospheric fields from the analysis and in the precipitation forecasts over parts of the tropics, and especially over West Africa, have been examined. Our experiments produce a moistening of the atmosphere over India, South America, and in West Africa together with a drying of the atmosphere over Saudi Arabia and northeast Africa. The drying or moistening of the atmosphere is far from being negligible and has been successfully evaluated using independent TCWV measurements from the GPS AMMA network.

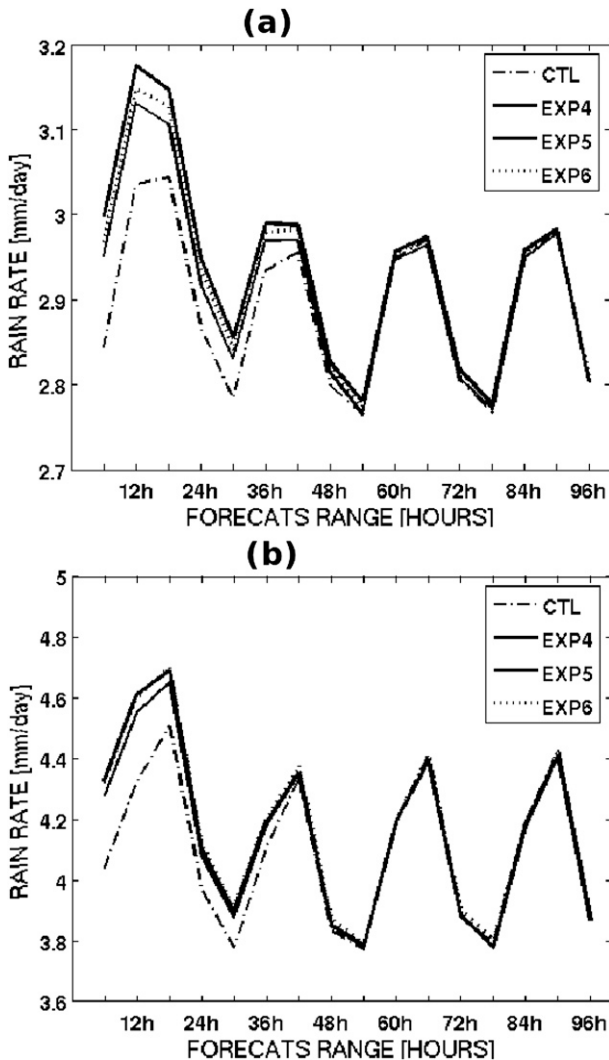


FIG. 18. Mean rain-rate forecasts (averaged over 45 days) as a function of the forecast range and as provided by CTL and EXP4–EXP6. Results are given for the (a) globe and (b) tropics.

It should be mentioned that very similar humidity features over the tropics have been observed when assimilating TCWV from Medium Resolution Imaging Spectrometer (MERIS) observations over land (Bauer 2009). Additional assimilation experiments with a better use of MERIS and AMSU observations over land have been run using the latest version of the ECMWF assimilation system and will be described in a forthcoming paper. In relation to the humidity change (experiment minus CTL) over the tropics, the humidity dipole over West Africa has been strengthened, resulting in an increase in the low-level baroclinicity. All together, this results in a better-organized African monsoon with an intensification of the deep ascent in the ITCZ with more precipitation, whereas the shallow forced ascent at the ITD is reduced.

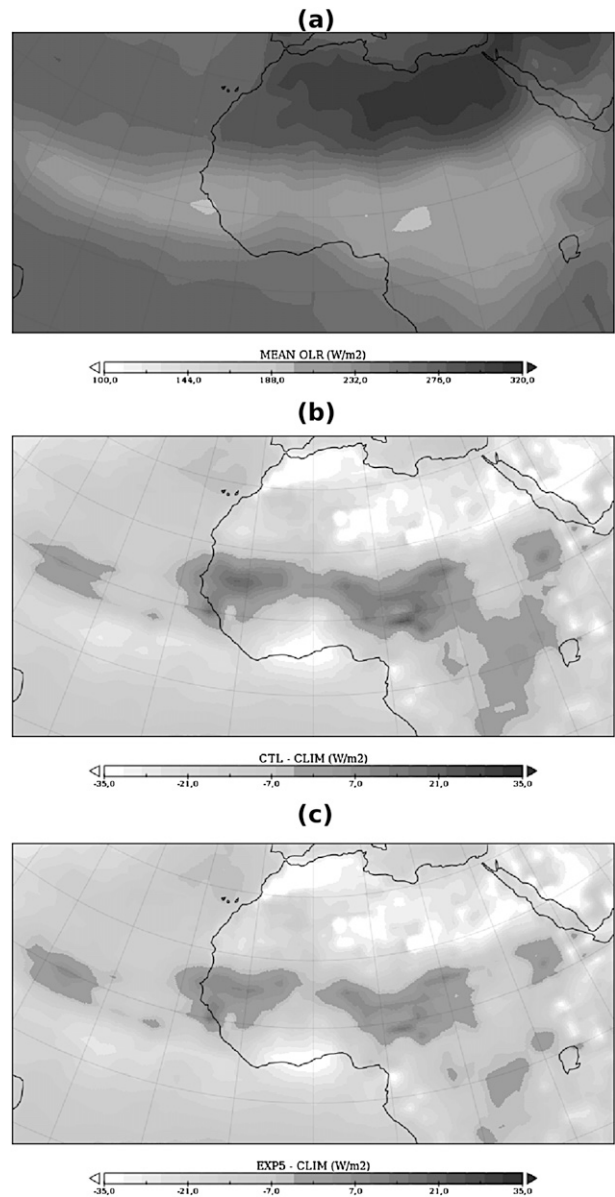


FIG. 19. (a) Main OLR estimates from NCAR during August 2006 and the average of the 24-h cumulated OLR using forecasts from (b) CTL and (c) EXP5.

In addition, the AEJ is intensified over Sudan at its entry zone, which modifies the AEW activity. Globally, the moistening does not result in a northward shift of the monsoon system, probably due to stabilization effects.

Considering short-range precipitation forecasts, the assimilation of humidity observations from AMSU-B decreases the precipitation over tropical oceans (especially the eastern Atlantic) and increases it over the continents. The assimilation reduces a well-known deficiency of most of the models. Over Africa we note three zones of rainfall increase: near the Guinean coast,

the west coast, and the Ethiopian Highlands. However, we have noticed the so-called spindown problem, which is characterized by an increase in the rainfall during the first day of the forecast. Such a problem cannot be solved unless more significant changes are made to the moist physics parameterization to improve the model equilibrium and bring it closer to the observations. Short-range OLR forecasts have been compared with independent OLR estimates and the comparison was in favor of experiments assimilating microwave observations over land.

Finally, let us point out that our assimilation experiments should be considered as first trials even if very promising results have been obtained. Further studies toward the assimilation of significantly more observations in clear, as well as cloudy, conditions are planned. With regard to the major changes to key parameters of the water cycle brought about by the present assimilation scheme, we strongly recommend that joint studies on the physical parameterization of the models be undertaken. Current work is on going in comparing the impacts of this assimilation upon different model systems.

Acknowledgments. The authors would like to deeply thank three anonymous reviewers for their numerous constructive insights; their suggestions greatly improve the manuscripts. We wish to thank Jean Maziejewski for his help in revising the manuscript. The authors thank Francois Bouyssel for fruitful discussions about the assimilation of humidity observations. The authors are grateful to Alan Geer for his help with IDL routines.

Based on a French initiative, AMMA was built by an international scientific group and is currently funded by a large number of agencies especially from France, United Kingdom, United States, and Africa. This project has been the recipient of an important financial contribution from the European Community's Sixth Framework Research Program. Detailed information on the scientific coordination involved with this program is available on the AMMA international Web site (<http://www.amma-international.org>). Interpolated OLR data used in this study have been provided by the NOAA/OAR/ESRL PSD, Boulder, Colorado, from their Web site (<http://www.cdc.noaa.gov>).

REFERENCES

- Bauer, P., 2009: 4D-Var assimilation of MERIS total column water vapour retrievals over land. *Quart. J. Roy. Meteor. Soc.*, **135**, 1852–1862.
- , P. Lopez, A. Benedetti, D. Salmond, M. Bonazzola, and S. Saarinen, 2006a: Implementation of 1D + 4D-Var assimilation of microwave radiances in precipitation at ECMWF. Part I: 4D-Var. *Quart. J. Roy. Meteor. Soc.*, **132**, 2277–2306.
- , —, —, —, —, and —, 2006b: Implementation of 1D + 4D-Var assimilation of microwave radiances in precipitation at ECMWF. Part II: 4D-Var. *Quart. J. Roy. Meteor. Soc.*, **132**, 2307–2332.
- Bock, O., M. N. Bouin, A. Walpersdorf, J.-P. Lafore, S. Janicot, F. Guichard, and A. Agusti-Panareda, 2007: Comparison of ground-based GPS precipitable water vapour to independent observations and NWP model reanalyses over Africa. *Quart. J. Roy. Meteor. Soc.*, **133**, 2011–2027.
- Courtier, P., J. N. Thépaut, and A. Hollingsworth, 1994: A strategy for operational implementation of 4D-Var using an incremental approach. *Quart. J. Roy. Meteor. Soc.*, **120**, 1321–1387.
- Grody, N. C., 1988: Surface identification using satellite microwave radiometers. *IEEE Trans. Geosci. Remote Sens.*, **26**, 850–859.
- Karbou, F., E. Gérard, and F. Rabier, 2006: Microwave land emissivity and skin temperature for AMSU-a and -b assimilation over land. *Quart. J. Roy. Meteor. Soc.*, **132**, 2333–2355.
- , —, and —, 2010: Global 4DVAR assimilation and forecast experiments using AMSU observations over land. Part I: Impacts of various land surface emissivity parameterizations. *Wea. Forecasting*, **25**, 5–19.
- Leroux, S., and N. M. J. Hall, 2009: On the relationship between African easterly waves and the African easterly jet. *J. Atmos. Sci.*, **66**, 2303–2316.
- Liebmann, B., and C. A. Smith, 1996: Description of a complete (interpolated) outgoing longwave radiation dataset. *Bull. Amer. Meteor. Soc.*, **77**, 1275–1277.
- Rabier, F., H. Jarvinen, E. Klinker, J. F. Mahfouf, and A. Simmons, 2000: The ECMWF operational implementation of four-dimensional variational assimilation. I: Experimental results with simplified physics. *Quart. J. Roy. Meteor. Soc.*, **126**, 1143–1170.
- Redelsperger, J.-L., C. Thorncroft, A. Diedhiou, T. Lebel, D. Parker, and J. Polcher, 2006: African Monsoon Multidisciplinary Analysis: An international research project and field campaign. *Bull. Amer. Meteor. Soc.*, **87**, 1739–1746.
- Veersé, F., and J. N. Thépaut, 1998: Multiple truncation incremental approach for four-dimensional variational data assimilation. *Quart. J. Roy. Meteor. Soc.*, **124**, 1889–1908.
- Weng, F., B. Yan, and N. Grody, 2001: A microwave land emissivity model. *J. Geophys. Res.*, **106**, 20 115–20 123.
- Zhang, C., P. Woodworth, and G. Gu, 2006: The seasonal cycle in the lower troposphere over west Africa from sounding observations. *Quart. J. Roy. Meteor. Soc.*, **132**, 2561–2584.